Evaluation of data from direct numerical simulations of transition due to free-stream turbulence

By Robert G. Jacobs AND Dan S. Henningson[1]

1. Motivation and objectives

The effect of free-stream turbulence (FST) on the onset of transition has only recently received detailed attention although FST is one of the important sources leading to by-pass transition. Such disturbances are of great interest in engineering, for instance for the prediction of transition on turbine blades, where the impingement of turbulence from the wake of the stator influences the boundary layers on the rotor blades. Another important aspect is the influence of FST on wind-tunnel experiments in general. It is desirable to reduce the FST-level in order to resemble free-flight conditions, but all wind-tunnels have some background disturbances with different characteristics, and knowledge about the 'dangerous' FST- parameters is of interest. Attempts have been made to establish empirical correlations between the free-stream turbulence and the transition Reynolds number. At FST levels (Tu) above 5-10%, transition occurs at the minimum Reynolds number where self-sustained boundary layer turbulence can exist, i.e. at $Re_\theta \approx 190$ where Re_θ denotes the Reynolds number based on momentum loss thickness (see Arnal, 1987, for a review). At lower levels of FST, however, the results are less clear.

1.1 The Klebanoff mode

The effect of free-stream turbulence on the onset of transition was first investigated by Klebanoff (1971). Kendall (1985) summarizes the results as follows:

"Klebanoff recorded the fluctuation development in a flat plate layer at Re_x up to $2.1 \cdot 10^6$ for stream turbulence levels up to 0.3 percent. The turbulence was generated by means of various grids placed in the settling chamber of the tunnel. He showed that low frequency (in comparison with the most amplified TS-waves) fluctuations commenced growth at the plate leading edge and attained an amplitude of five percent at a station well ahead of the onset of transition, with the amplitude along the plate length varying in direct proportion to the boundary layer thickness."

"The broad band signal amplitude distribution through the layer resembled that which would result from a thicken/thinning oscillation of the layer, and Klebanoff referred to the low frequency motion as the breathing mode of the layer. He found by correlation methods that the broadband disturbances were quite narrow laterally, being no more than a few boundary layer thicknesses wide, although the scale depended upon that of the free-stream turbulence and not upon the layer thickness."

1 The Aeronautical Research Institute of Sweden (FFA), Box 11021, S-16111 Bromma, Sweden, and Department of Mechanics, KTH, S-10044 Stockholm, Sweden

Kendall named this new disturbance type a Klebanoff mode. This summarizes the main features of the effect of FST on a boundary layer, and in the work by Kendall additional details of the disturbances are given. In flow visualizations, for example, he shows that these low-frequency oscillation are associated with long streaky structures inside the boundary layer.

1.2 Direct numerical simulations

The simulations evaluated here were performed by Jacobs (1999). The incompressible Navier-Stokes equations were solved by the fractional step algorithm described in Akselvoll & Moin (1995). This is a central difference, pressure correction method, solved on a staggered grid. Convection and diffusion in the horizontal plane are treated explicitly and solved by third order Runge-Kutta time stepping. Diffusion is implicit in the vertical direction, and convection is linearized to make it partially implicit. The implicit terms follow the Crank-Nicholson time-stepping scheme. The computer code is a parallel implementation of this algorithm by Pierce & Moin (1998). Computations were done on 128 processors of an SGI Origin 2000. A full simulation required on the order of 500 hours of CPU time per processor.

The flow domain was a rectangular box of relative dimensions 15.5 x 1 x 0.75. The grid was uniformly spaced in the x and z-directions and clustered near the wall in the wall-normal direction. The uniform grid spacing in the horizontal plane enabled the Poisson equation for the pressure to be solved directly by Fourier transforms in x and z with a tri-diagonal matrix inversion in y.

2. Comparison of DNS data with experiments

Simulations were run for FST inlet intensities of 3.5% and 7% and are termed Case 1 and 2, respectively. These intensities were chosen to correspond loosely with the T3A and T3B experimental studies of Roach & Brierley (1992). The solutions presented herein are from Case 1 on a 2048 x 180 x 192 grid which gives $\Delta x^+ = 11.7$ and $\Delta z^+ = 6.0$ at the skin friction maximum. More details can be found in Jacobs (1999).

A plot of skin friction coefficient versus Reynolds number provides a good overview of the onset and length of transition. The development of the skin friction coefficient are shown in Fig. 1. The data of Roach & Brierley (1992) are included for comparison. Mean velocity profiles at various locations in the transitional and turbulent regions are compared to experimental data in Fig. 2.

2.1 Overview of the flow structures

The investigations of Klebanoff and Kendall are done with rather low freestream turbulence levels, $Tu < 1\%$, where Tu is in measurements usually set equal to u_{rms}/U_∞ in the freestream. The same streaky disturbances continue to be the main flow features as the free-stream turbulence level increases. In Fig. 3 a smoke visualization of a boundary layer subjected to a FST level of 6% can be seen to have the typically streaky appearance. Detailed studies of flow visualizations show that breakdown to turbulent spots occurs in regions where strong streaks exist. The transition region is then characterized by a random appearance of turbulent spots,

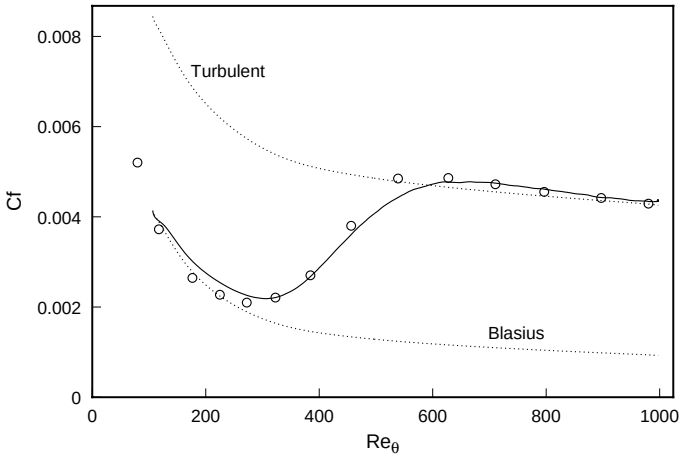

FIGURE 1. Skin friction versus Reynolds number based on downstream location compared to data of Roach & Brierley (1992). ○ : T3A; ——— : Case 1.

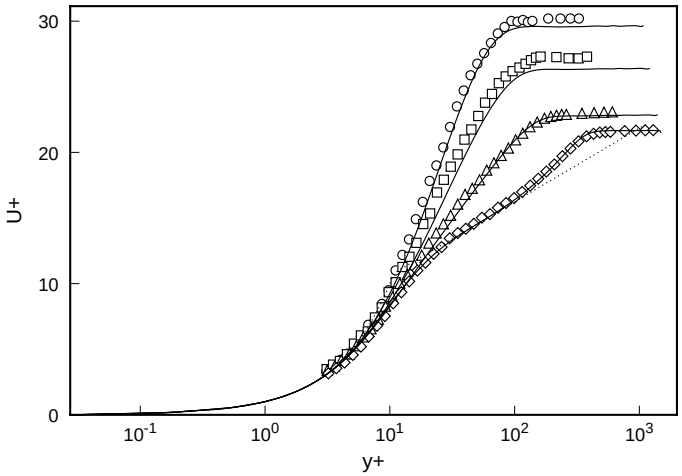

FIGURE 2. The evolution of mean streamwise velocity profiles compared to data of Roach & Brierley (1992). ○ $Re_\theta = 323$; □ $Re_\theta = 385$; △ $Re_\theta = 456$; ◇ $Re_\theta = 980$. Corresponding profiles from Jacobs Case 1 (———). The log law is denoted by ····· .

which grow in number and size downstream until the boundary layer becomes fully turbulent.

In the simulations shown in Fig. 4, the instantaneous streamwise fluctuation velocity in a horizontal plane is seen both inside and outside the boundary layer. At the inflow small scale turbulent fluctuations are seen at both positions. Above the boundary layer the intensity of the turbulence is seen to slowly decay downstream from an initial intensity of about $Tu = 3\%$. Inside the boundary layer the turbulence is highly damped, and the same streaky structures seen in the smoke visualizations appear. As the streaks are followed downstream, they can be seen to break down to a turbulent flow through the formation of turbulent spots. Thus the simulations and

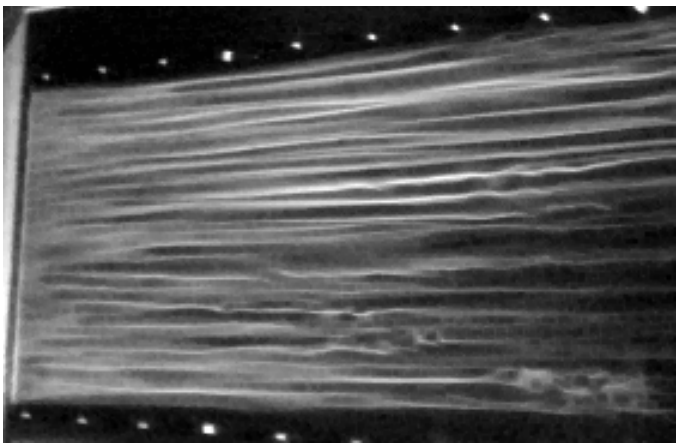

FIGURE 3. Streaky structures observed through smoke visualization in a laminar boundary layer subjected to 6% free-stream turbulence. Flow from left to right. Note the sign of streak oscillations and breakdown at the downstream end of the photograph. From Alfredsson & Matsubara (1996).

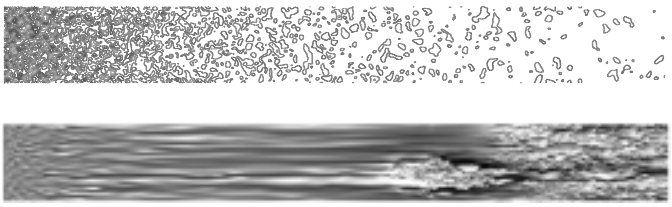

FIGURE 4. Contours of the streamwise velocity above (top) and inside (bottom) the boundary layer. $Re_\theta = 107$ at the inflow.

the experiments give the same overall picture of the transition process in boundary layers subjected to moderate levels of free-stream turbulence.

2.2 Velocity measurements and correlations

Velocity signals from the numerical simulations are shown in Fig. 5. It shows that the high frequencies in the free-stream turbulence rapidly damp in the boundary layer while the low frequencies amplify. Similar hot-wire measurements are presented by Alfredsson & Matsubara (1996) and Westin *et al.* (1994) for $Tu = 1.5\%$ (see e.g. Fig. 6). It is the streaks that give rise to low frequency disturbances when the streamwise velocity is measured by a stationary hot wire inside the boundary layer. The energy spectrum inside the boundary layer is dominated by contributions at much lower frequencies than in the turbulent freestream.

Westin *et al.* (1994) shows that although the u_{rms} levels inside the boundary layer may reach 10% or more before transition to turbulence occurs, the boundary layer profile is only slightly changed as compared to the undisturbed flow. The rms-profiles for both u and v are shown in Fig. 7 for four downstream positions. It is clearly shown how the intensity increases in the downstream direction and that u_{rms} has a maximum in the center of the boundary layer. The level of v_{rms} starts

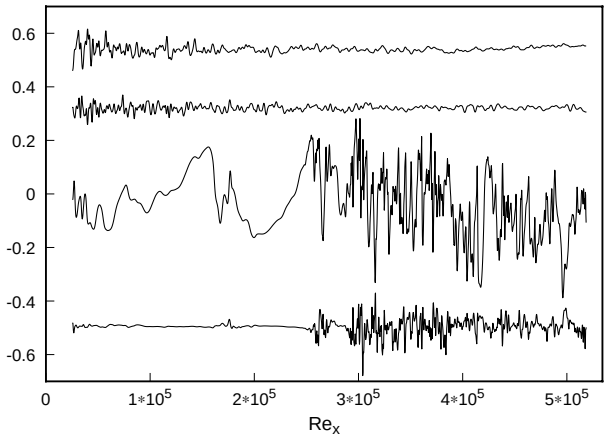

FIGURE 5. Velocity signals inside and outside the boundary layer. The upper pair of traces are u and v in the freestream. The bottom pair of traces are u and v in the boundary layer at approximately $y/\delta^* = 1.5$.

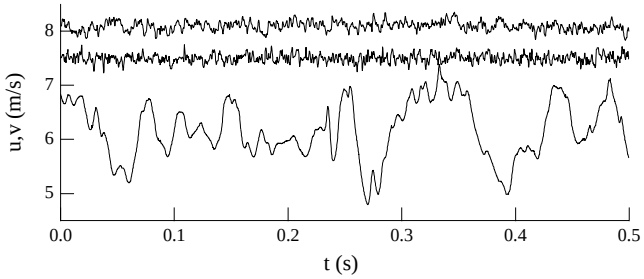

FIGURE 6. Comparison between velocity signals inside and outside a boundary layer subjected to FST. The upper two traces are u and v measured in the freestream, whereas the lower trace is u measured at $y/\delta^* = 1.5$. From Alfredsson & Matsubara (1996).

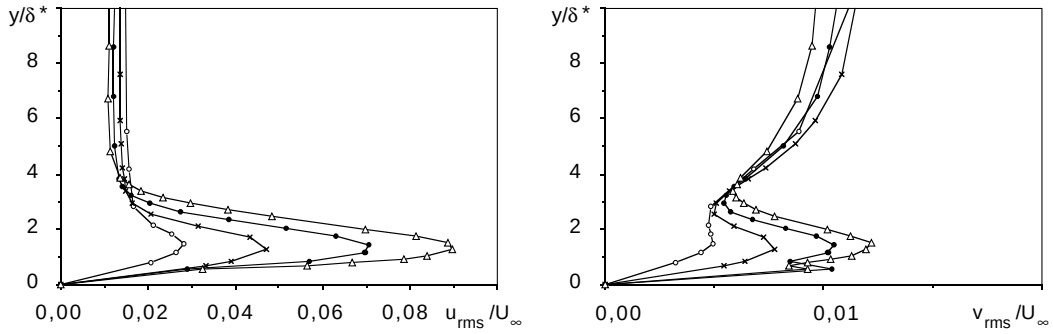

FIGURE 7. u_{rms} and v_{rms}-profiles for four different downstream positions in a boundary layer subjected to FST. o: $x = 100mm$, $\times$: $x = 250mm$, $\bullet$: $x = 500mm$, Δ: $x = 800mm$. Note different scales. From Alfredsson & Matsubara (1996).

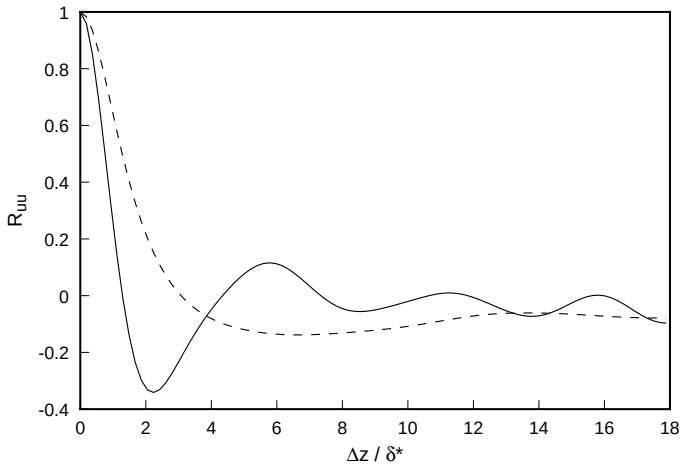

FIGURE 8. Spanwise correlation of streamwise velocity fluctuation at $Re_\theta = 307$ with spanwise length scale normalized by the displacement thickness. ——— $y/\delta = 0.5$; — — — freestream.

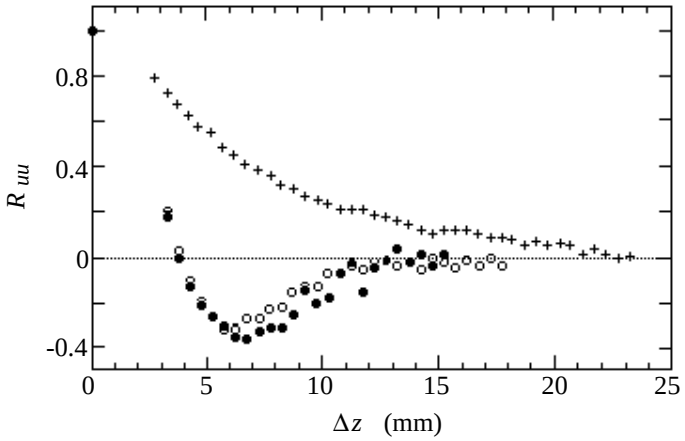

FIGURE 9. Spanwise correlations in the boundary layer, measured close to the maximum of u_{rms} for $x = 500mm$ (○), $x = 1000mm$ (●). Spanwise correlation in the freestream at $x = 500mm$ (+). From Westin *et al.* (1994).

to decrease from its free-stream value towards the wall already several boundary layer thicknesses from the wall.

The spanwise distribution of the boundary layer perturbations in Figs. 8 and 9 is illustrated by the correlation between two velocity signals displaced in the spanwise direction. There is a clear anti-correlation at a certain spanwise separation, approximately the size of the boundary layer thickness, corresponding to half of the averaged spacing of the streaks.

2.3 The origin of streaks

Profiles from the simulations are included in Fig. 10, which can be compared to the results from the calculations of the optimal streak growth of Andersson *et al.*

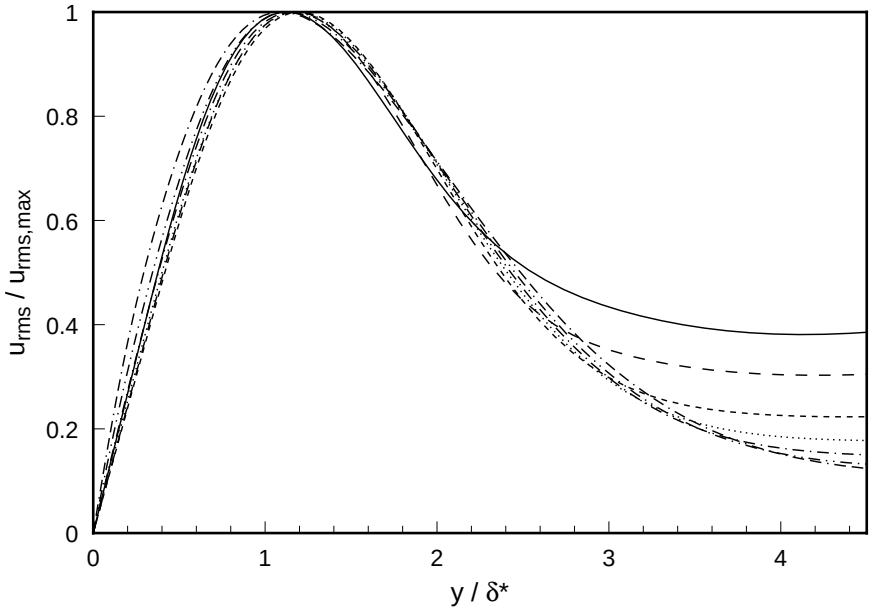

FIGURE 10. Streamwise turbulence intensity normalized by the maximum intensity versus wall-normal distance normalized by the local displacement thickness. ——— $Re_{\delta*} = 337$; — — — $Re_{\delta*} = 371$; - - - - $Re_{\delta*} = 438$; ····· $Re_{\delta*} = 483$; —·— $Re_{\delta*} = 537$; —··— $Re_{\delta*} = 578$; - - ·· - - $Re_{\delta*} = 621$.

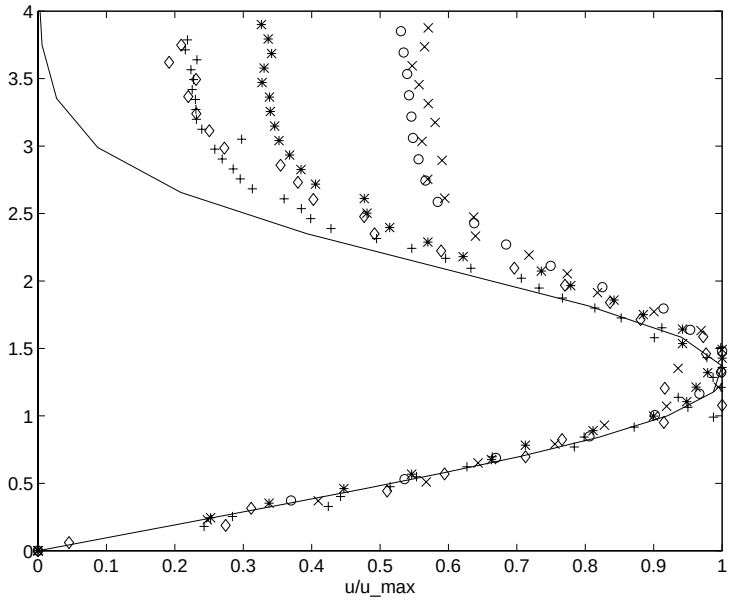

FIGURE 11. Comparison between the streamwise velocity component of the downstream response of an optimal perturbation and experimental data. In the calculations the parameters used were $x_f = 1$, $x_0 = 0$, $\beta = 0.45$, and Re $> 10^6$. ——— theory; ∘ $R_{\delta*} = 350$; × $R_{\delta*} = 400$; * $R_{\delta*} = 525$; + $R_{\delta*} = 715$; ◇ $R_{\delta*} = 890$. From Andersson *et al.* (1999).

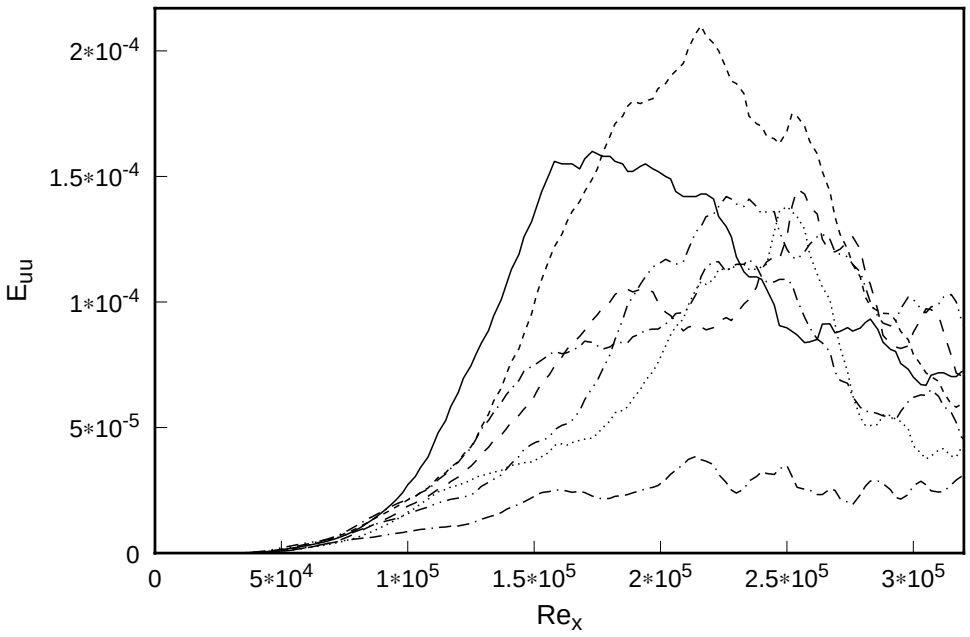

FIGURE 12. Maximum energy in the boundary layer in the streamwise velocity frequency spectra at $\beta\delta_0 = 1.2$. ——— F = 3; — — — F = 6; - - - - F = 9; ····· F = 12; —·— F = 15; —··— F = 18; - - ·- - F = 51.

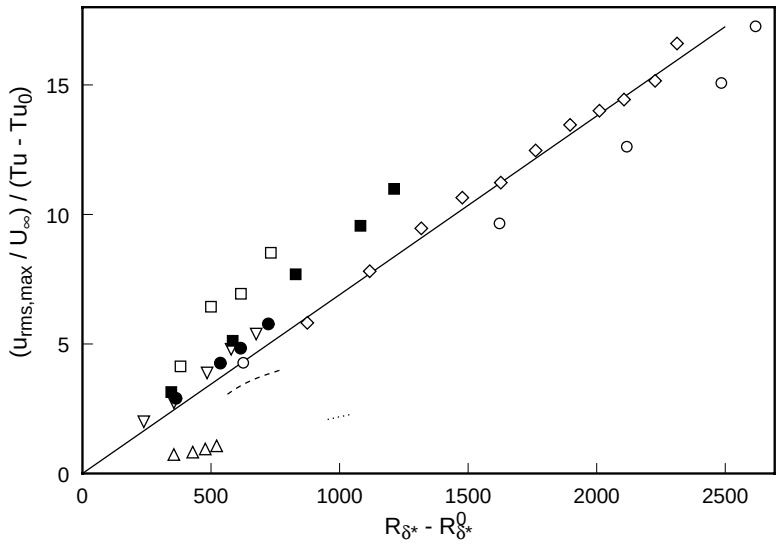

FIGURE 13. Comparisons of downstream growth of $u_{rms,max}$ with Re_{δ^*} in various experiments. ○ Arnal & Juillen, Tu = 0.85%; □ Kosorygin *et al.*, Tu = 1.4%; △ Kosorygin *et al.*, Tu = 3.2%; ◇ Roach & Brierley, Tu = 1.0%; ▽ Roach & Brierley, Tu = 3.0%; ● Westin *et al.*, Tu = 1.35%; ■ Westin *et al.*, Tu = 1.5%; - - - - Jacobs, Tu = 3.5%; ····· Jacobs, Tu = 7.0%.

in Fig. 11. In the latter figure the optimal streak is plotted together with experimental data from Westin *et al.* The experimental data represent profiles of root-mean-square streamwise velocity perturbations seen in Fig. 7. In both numerical simulations and experiments, the typical shape of the Klebanoff mode appears.

Data from the simulations in Fig. 12 show the maximum energy inside the boundary layer at a given spanwise wavenumber at several frequencies. This shows that it is the lower frequencies which are responsible for the initial growth of perturbations. This is in agreement with e.g. the data of Kendall presented by Bertolotti (1997).

The maximum energy growth calculated by Andersson *et al.* (1999) scaled linearly with downstream distance. This implies that the amplitude growth scales linearly with the Reynolds number based on displacement thickness. Figure 13 shows the downstream growth of u_{rms} with Re_{δ^*} in a number of different experiments. Here we have also included the experiments of Kosorygin *et al.* (1982) and Arnal & Juillen (1978). The u_{rms} is scaled with $(Tu - Tu_0)U_0$, where $Tu_0 = 0.5\%$ and Re_0 is chosen so that the full line passes through the origin. It is interesting to note the linear collapse of the data and that $Tu = 0.5\%$ is approximately the value below which the streak breakdown scenario ceases to exist. Westin *et al.* (1994) showed a similar plot, but with $Tu_0 = Re_0 = 0$, and were not able to collapse the data. The linear growth seen here was used by Andersson *et al.* (1999) to construct a simple transition prediction method able to correlate the free-stream turbulence level with the transition location in a number of experiments.

The good agreement between the measured and calculated velocity profiles as well as the approximately linear growth of the streak energy with downstream distance predicted by theory, experiment, and simulation indicate that the streaks captured by the model of Andersson *et al.* are the Klebanoff modes. Indeed, it also indicates the origin of the Klebanoff mode as a streamwise vortex situated outside the boundary layer at the leading edge. However, there are other possible sources of the boundary layer streaks. Berlin *et al.* (1999) showed that oblique disturbances in the freestream could easily generate streamwise vortices and subsequent streaks inside the boundary layer. This is a non-linear process and is most likely active for higher levels of free-stream turbulence.

REFERENCES

Akselvoll, K. & Moin, P. 1995 Large eddy simulation of turbulent confined coannular jets and turbulent flow over a backward facing step. *Report No. TF-63.* Stanford University, Thermosciences Division.

Alfredsson, P. H. & Matsubara, M. 1996 Streaky structures in transition. In *Transitional Boundary Layers in Aeronautics.* Henkes, R. & van Ingen, J., eds., Elsevier Science Publishers, 374-386.

Andersson, P., Berggren, M. & Henningson, D. 1999 Optimal disturbances and bypass transition in boundary layers. *Phys. Fluids.* **11**(1), 134-150.

Arnal, D. 1987 Transition description and prediction. In *Numerical simulation of unsteady flows and transition to turbulence.* Pironneau, O., Rodi, W., Ryhming,

I., Savill, A. & Truong, T., eds., Cambridge University Press, 303-316.

Arnal, D. & Juillen, J. 1978 Contribution experimentale a l'etude receptivite d'une couche limite laminaire, a la turbulence de l'ecoulement general. *ONERA Rapport Technique No 1/5018 AYD.*

Berlin, S. & Henningson, D. S. 1999 A new nonlinear mechanism for receptivity of free-stream disturbances. To appear in *Phys. Fluids.*

Bertolotti, F. P. 1997 Response of the Blasius boundary layer to free-stream vorticity. *Phys. Fluids.* **9**(8), 2286-2299.

Jacobs, R. 1999 A Study of bypass transition phenomena by computer simulation. *PhD thesis,* Department of Mechanical Engineering, Stanford University.

Kendall, J. M. 1985 Experimental study of disturbances produced in a pretransitional laminar boundary layer by weak freestream turbulence. *AIAA Paper 85-1695.*

Klebanoff, P. S. 1971 Effect of freestream turbulence on the laminar boundary layer. *Bull. Am. Phys. Soc.* **10,** 1323.

Kosorygin, V., Polyakov, N., Suprun, T. & Epik, E. 1982 Development of disturbances in the laminar boundary layer on a plate at a high level of free stream turbulence (in Russian). In *Instability of subsonic and supersonic flows.* 85-92.

Pierce, C. D. & Moin, P., 1998 Large eddy simulation of a confined coaxial jet with swirl and heat release AIAA 98-2892, 29th AIAA Fluid Dynamics Conference, June 15-18 Albuquerque, New Mexico.

Roach, P. E. & Brierley, D. H. 1992 The influence of a turbulent free-stream on zero pressure gradient transitional boundary layer development. In *Numerical Simulations of Unsteady Flows and Transition to Turbulence,* Cambridge University Press. 319-347.

Westin, K. J. A., Boiko, A. V., Klingmann, B. G. B., Kozlov, V. V. & Alfredsson, P. H. 1994 Experiments in a boundary layer subject to free-stream turbulence. Part I: Boundary layer structure and receptivity. *J. Fluid Mech.* **281,** 193-218.